

Temporal left atrial lesion formation following ablation of atrial fibrillation: Lessons learned from delayed enhancement MRI

Troy J. Badger MD ¹, Robert S. Oakes ¹, Marcos Daccarett MD ¹, Nathan S. Burgon BS ¹, Nathan M. Segerson MD ¹, Nazem Akoum MD ¹, Eric N. Fish ¹, Swati N. Rao ¹, Joshua J.E. Blauer BS ^{1,3}, Eugene G. Kholmovski PhD ², Sathya Vijayakumar MS ², Edward V.R. Di Bella PhD ², Rob S. MacLeod PhD ³ and Nassir F. Marrouche MD ¹

¹ Atrial Fibrillation Program - Division of Cardiology, University of Utah School of Medicine. Salt Lake City, Utah.

² Utah Center for Advanced Radiology Research, University of Utah. Salt Lake City, Utah.

³ Scientific Computing Institute, University of Utah. Salt Lake City, Utah.

Corresponding Author

Nassir F. Marrouche, MD
Director, Cardiac Electrophysiology Laboratories
Director, Atrial Fibrillation Program

Division of Cardiology
University of Utah Health Sciences Center
30 North 1900 East
Room 4A100
Salt Lake City, Utah 84132-2400

Nassir.Marrouche@hsc.utah.edu

Phone: +1-801-581-2572

Fax: +1-801-581-7735

Abstract

Background. Pulmonary vein antrum isolation (PVAI) uses radiofrequency (RF) energy to induce thermal damage to the left atrial (LA) substrate in an attempt to isolate atrial fibrillation (AF) circuits. This LA tissue injury can be seen using delayed enhancement MRI (DE-MRI).

Methods. A group of twenty-five patients who presented for PVAI were scanned serially at two different time points. The first group (n = 10) of patients had DE-MRI acquired twenty four hours and three months following PVAI. The second group (n = 16) were scanned three months and six months following PVAI. Three dimensional models of the LA were created and analyzed to determine structural change. The extent of scar formation was analyzed using an automated computer algorithm based on dynamic thresholding.

Results. The median change in LA wall injury between 24 hours and 3 months (Group 1) was -6.38% (range = -11.7% to 12.58%). The median change in LA wall injury between 3 months and later follow-up (Group 2) was +2.0% (range = -4.0% to 6.58%). Qualitative comparison of LA scar patterns revealed a stronger qualitative relationship between MRI scans acquired at 3 months and later follow-up than at 24 hours and 3 months. There appears to be little relationship between the extent of scar at 24 hours and that detected at three months ($R^2 = 0.004$). In contrast, a strong correlation is seen at 3 months and later follow-up ($R^2 = 0.966$).

Conclusion. RF-induced scar as measured by DE-MRI following PVAI appears to have formed by three months post-ablation. Scar patterns remain consistent in their extent, location and intensity at later follow-up. At 24 hours following the procedure, DE-MRI enhancement appear consistent with a transient inflammatory response rather than stable LA scar formation.

Background

Catheter ablation has emerged as a promising interventional treatment for atrial fibrillation (AF) patients who have failed anti-arrhythmic or rate control therapy.¹⁻⁴ Many of the current ablation techniques, including Pulmonary Vein Antrum Isolation (PVAI), use high-frequency RF energy to induce thermal damage to the left atrial (LA) substrate in attempt to electrically disconnect and isolate arrhythmogenic foci originating from the pulmonary vein.⁵⁻⁷ Energy delivery causes contraction band myocardial necrosis followed by inflammatory infiltrates that results in fibrotic scarring of the LA wall.⁸⁻¹²

Until recently, no modality other than histological preparation of tissue has allowed for the analysis of scar formation following RF ablation, and this has been limited only to post-mortem specimens. However, new techniques have led to the use of delayed-enhancement MRI (DE-MRI) to visualize RF-induced scar formation in AF patients post-ablation.^{13, 14} DE-MRI utilizes differences in the washout kinetics of the contrast agent gadolinium to differentiate between healthy and injured myocardial tissue. These scans can be rendered as three-dimensional models of the LA which show post-ablation scar patterns near the pulmonary vein ostia and posterior wall.^{14, 15}

Although visualization of LA wall damage is now possible, the process of scar formation following AF ablation is still poorly understood. There is no knowledge of how LA lesions appear in size, intensity and location in the acute and chronic post-ablation stages and the manner which their morphology changes over time. Prior work has shown that AF often recurs in patients who recover conduction between the pulmonary veins and the LA.¹⁶ Closing conduction gaps on repeat procedure has successfully eliminated the arrhythmias.¹⁷ Therefore, understanding the temporal process of scar formation and whether scar significantly reduces or expands over time may be valuable in determining

whether certain patients are more susceptible to recovery of electrical conduction and a subsequent recurrence of AF.

In this study, we examine ablation-induced scar and how it responds over time. We evaluated LA lesions utilizing DE-MRI in two separate groups of AF patients; the first group had scans acquired at 24 hours post-procedure and 3 months post procedure. The second had scans acquired at 3 months post procedure and at 6 or 9 months post procedure. The results presented here provide important insight to the healing process following ablation of the left atrium and its subsequent remodeling.

Methods

Patients

Between November 2006 and January 2008, 25 patients with AF who presented to the University of Utah for PVAI of symptomatic AF were enrolled in this study. The protocol was approved by the Institutional Review Board at the University of Utah and was HIPAA compliant. Patients were eligible for the study if they underwent two DE-MRI scans at two different time points following their PVAI procedure. DE-MRI was obtained at either 24 hours, 3, 6, or 9 months post-ablation. All 25 patients received MRI at 3 months as a component of post-procedural follow-up care. MRI was obtained at 24 hours post procedure in 10 patients in order to assess for complications in symptomatic patients. The remaining 15 patients were imaged at 6 or 9 months as a component of routine follow-up care. 1 patient had images acquired at 24 hours, 3 months, and 9 months.

Prior to the PVAI procedure, all patients underwent transesophageal echocardiogram (TEE) in order to rule out LA appendage thrombus. Patients then underwent MRI to define left atrial anatomy, LA area and LA wall thickness for electroanatomical mapping during the ablation procedure, delayed enhancement scans were performed as a part of the MRI imaging protocol.

Delayed Enhancement MRI Acquisition

All patients underwent MRI studies on a 1.5 Tesla Avanto clinical scanner (Siemens Medical Solutions, Erlangen, Germany) using a TIM phased-array receiver coil 24 to 72 hours prior to PVAI. The protocol included sequences to define the anatomy of the LA and the pulmonary veins. The anatomy was evaluated by using the contrast enhanced 3D FLASH sequence and cine true-FISP sequences. Typical acquisition parameters for the 3D FLASH scan were: breath-hold in expiration, a transverse (axial) imaging volume with voxel size=1.25x1.25x2.5 mm, repetition time (TR) = 3.1 ms, echo time (TE) = 1.0 ms, and parallel imaging using the GRAPPA technique with reduction factor R=2 and 32 reference lines, scan time=14 sec. The 3D FLASH scan was acquired twice: pre-contrast and during a first pass of contrast agent (Multihance (Bracco Diagnostic Inc., Princeton, NJ), intravenous injection of a dose of 0.1 mmol per kilogram of body weight, 2 ml/sec injection rate, followed by a 30 ml saline flush). Timing of the first pass scan was defined using an MRI fluoroscopic scan. Complete coverage of the LA was achieved with 16-22 transverse 2D slices acquired during retrospective electrocardiogram (ECG) gated, cine pulse sequence. All the images were acquired during breath-hold in expiration (1 or 2 slices per breath hold depending on the subject's heart rate and tolerance to breath-holding) and were used to evaluate the LA morphology during the cardiac cycle. Typical scan parameters were: 6 mm slice thickness, no gap between slices, pixel size = 2.0 x 2.0 mm, TR/TE = 2.56/1.03 ms, GRAPPA with R=2 and 44 reference lines, 15 views per segment.

Delayed enhancement MRI (DE-MRI) was used to identify injured or nonviable tissue in the LA. DE-MRI was acquired about 15 minutes after the contrast agent injection using a 3D inversion recovery prepared, respiration navigated, ECG-gated, gradient echo pulse sequence. Typical acquisition parameters were: free-breathing using navigator gating, a transverse imaging volume with voxel size = 1.25 x 1.25 x 2.5 mm (reconstructed to 0.625 x 0.625 x 1.25 mm), TR/TE = 6.3/2.3 ms,

inversion time (TI) = 230-270 ms, GRAPPA with R=2 and 32 reference lines. ECG gating was used to acquire a small subset of phase encoding views during the diastolic phase of the LA cardiac cycle. The time interval between the R- peak of the ECG and the start of data acquisition was defined using the cine images of the LA. Fat saturation was used to suppress fat signal. The TE of the scan (2.3 ms) was chosen such that fat and water are out of phase and the signal intensity of partial volume fat-tissue voxels was reduced allowing improved delineation of the LA wall boundary. The TI value for the DE-MRI scan was identified using a scout scan. Typical scan time for the DE-MRI study was 5-10 minutes depending on subject respiration and heart rate. If the first acquisition of 3D DE-MRI did not have an optimal TI or had sub-optimal image quality, the scan was repeated.

Pulmonary Vein Antrum Isolation and Posterior Wall Debulking

The methods for pulmonary vein antral isolation under intracardiac echocardiogram (ICE) guidance have previously been described elsewhere.^{4, 18} We have modified this procedure to include debulking and isolation of the posterior wall. Though the rationale for and the description of this method is not the focus of this manuscript, the technique is briefly summarized below.

After venous access, a 14-pole coronary sinus catheter was placed into the coronary sinus via the right internal jugular access (TZ Medical Inc., Portland, OR, USA) for use as a mapping reference. A phased-array ultrasound catheter was positioned in the mid-right atrium (Siemens AG Inc., Malvern, PA, USA) and used to guide a double transseptal puncture, through which was placed a 10-pole Lasso catheter and an F-curve, Thermocool irrigated tip ablation catheter (Biosense Webster Inc).

Using fluoroscopy and electroanatomic mapping (CARTOMERGE, Biosense-Webster, Inc.) for catheter navigation, intracardiac potentials in the PV antra and on the posterior wall were mapped during sinus rhythm, and were targeted for ablation if fractionation was seen distinct from far-field atrial potentials. Lasso-guided RF delivery was performed, using Lasso electrogram artifacts to

confirm ablation catheter tip location relative to the substrate of interest. Lesions were delivered using 50 W with a 50°C temperature limit, for a duration of 10 to 15 seconds, with the endpoint being elimination of all high-frequency electrogram components. When all antral and posterior wall targets had been ablated, this entire region was re-surveyed for any return of electrical activity, and any such regions were retreated. In addition, entry block in all four pulmonary veins was confirmed with the ablation catheter after debulking was accomplished.

Post-ablation Management

After the PVAI, all patients were observed on a telemetry unit for 24 hours. Patients underwent 8 weeks of patient-triggered and auto-detected event monitoring. Eight-day Holter recordings were then obtained at 3 and 6 months. PVAI success was defined as a lack of symptoms and absence of AF or AFL on all ECG, Holter, and cardiac event monitoring.

Image Analysis

Three-Dimensional MRI Models

All MR images were processed into three-dimensional (3D) models of the LA and were evaluated in random order and analyzed without knowledge of the time point after ablation by two independent observers. Images were processed using the MRI DICOM formatted data sets in Osirix. LA data from 3D DE-MRI acquisitions were evaluated slice-by-slice by utilizing volume-rendering tools. Each image slice was segmented and volume rendered to allow for unique visualization of LA wall radiofrequency injury patterns. Smooth table opacity was then applied to better illuminate hyperenhanced regions for visualization purposes.

Percent Enhancement of LA Wall

The relative percent of LA wall enhancement was measured at the post-PVAI scans using a threshold

based lesion detection algorithm. In all images, the epicardial and endocardial borders were manually contoured using custom image display and then analyzed by software written in Matlab (The Mathworks Inc. Natick, MA). Normal and injured tissue were defined based on a bimodal distribution of pixel intensities within the LA wall. The first mode of lower pixel intensities was chosen as normal tissue. Injured tissue was defined at 3 standard deviations above the normal tissue mean pixel intensity. Regions defined as lesion were visualized independently to ensure appropriateness of lesion detection. In cases where the degree of enhancement detected by the automated algorithm was determined to be inaccurate by an expert trained to DE-MRI, the cut-off value was adjusted. In patients where the algorithm overestimated the degree of RF induced scar, the threshold value was adjusted from 3 to 4 standard deviations. In patients where the algorithm underestimated the degree of RF induced scar, the threshold value was adjusted from 3 to 2 standard deviations. The threshold was manually adjusted in one patient (from 3 to 4 standard deviations), where the algorithm appeared to overestimate the degree of scar. The number of voxels corresponding to scar was determined for each slice and then summed for the entire scan. The degree of enhancement was reported as a ratio of lesion volume to total LA wall volume.

Comparison of Enhancement Patterns at Different Time-Points

A complete 3D panel was created for all patients, with image views of the posterior wall, septum, and free wall. A set of two trained experts qualitatively assessed and graded the relationship between the enhancement seen on both the first and second MRI time points. The relationship was rated on a 0 to 4 scale where 0 was coded as “No Relationship,” 1 was coded as “Poor”, 2 was graded as “Moderate,” 3 as “Good” and 4 as “Excellent Relationship.” The reviewers assessed the correlation of LA enhancement patterns in regards to size, location and intensity of the scar between both time points.

Statistical Analysis

Continuous variables are presented as median and the range. Continuous data was analyzed by Wilcoxon ranked sums test to measure for statistically significant differences. Fisher exact tests were used to test for differences in categorical measurements due to the small size of the cohort.

Differences were considered significant at $p < 0.05$. Statistical analysis was performed using the SPSS 15.0 Statistical Package (SPSS Inc.; Chicago, IL).

Results

Patient Group 1 – Delayed Enhancement MRI

Following ablation, all patients showed detectable hyperenhancement in the LA. However, there was substantial qualitative differences between the type of enhancement seen in patients at 24 hours when compared to all other time points (including 3, 6 and 9 month patient scans). Delayed enhancement at 24 hours appear less intense and more diffuse in nature. Three dimensional reconstructions show the same sort of diffuse enhancement patterns seen in two dimensions. Figure 1 shows the two dimensional and three dimensional enhancement patterns in one patient at 24 hours and 3 months following the PVAI. The characteristic pattern of diffuse, patchy enhancement (top) is clearly visible. Further, the overall intensity of the enhancement is less. In contrast, the scan at three months shows well-connected, well defined regions of intense enhancement in regions targeted during the ablation. Pulmonary vein isolation can be noted, which cannot be completely identified at twenty four hours.

Patient Group 2 – Delayed Enhancement MRI

MRI scans taken at later points of follow-up (6 or 9 months) show enhancement patterns similar to those acquired at three months. Figure 2 shows an example of two dimensional and three dimensional enhancement patterns in a second patient at three months and then later at six months following the

PVAI. The MRI obtained at three months shows scar patterns that remain consistent to the MRI obtained at 9 months. As evident in the three dimensional reconstructions showing all views of the LA, the overall intensity, location, and extent of ablation scarring are similar between the two MRI scans. Ablation scar around the pulmonary veins and posterior wall shows no significant change between the two time points.

DE-MRI Quantification and Qualitative Assessment

At twenty-four hours, the median LA wall injury was 9.9% of the LA myocardium (range = 7.20% to 19.80%). At three months (in Group 1 and Group 2) the median LA wall injury was 13.6% (range = 1.58% to 64.5%). The median patient change in LA wall injury between 24 hours and 3 months (Group 1) was -6.4% (range = -11.7% to 12.6%). The median patient change in LA wall injury between 3 months and later follow-up (Group 2) was 2.0% (range = -4.0% to 6.6%). This difference was consistent with patterns seen during manual assessment of the MRI images, specifically, that a general decrease in the degree of overall LA enhancement occurred from 24 hours to 3 months, while the degree of enhancement remained constant at three months to later follow-up periods. Figure 3 shows the range and inter-quartile range of both groups. The difference between Group 1 and Group 2 was statistically significant ($p = 0.048$, Wilcoxon Ranked Sums Test).

The qualitative comparison of the LA scar patterns between 24 hour and 3 months (Group 1) and 3 months and later follow-up (Group 2) revealed a stronger qualitative relationship among MRI scans acquired from 3 months to later time points. Figure 4 shows the distribution for the qualitative assessment score. The relationship between MRI scans in Group 1 were significantly lower than those in Group 2 ($p < 0.001$, Wilcoxon Ranked Sums Test). Figure 4 (Patient 1) shows an example of the 24 hour scar pattern which is diffuse (left) and which dramatically reduces at 3 months. In contrast,

Patient 2 shows an example where the LA posterior wall scar patterns remain consistent in size and location from 3 months on.

Figure 5 shows the results of pairwise regression analysis between the detected scar formation at 24 hours and 3 months (Group 1) and that at 3 months and later follow-up (6 or 9 months; Group 2). There appears to be no relationship between the overall scar extent at 24 hours and that detected later at three months ($R^2 = 0.0004$). In contrast, a strong correlation is seen between detected injury at 3 months and later follow-up ($R^2 = 0.966$).

Discussion

Our study is the first analysis to detail the morphological changes of RF-induced tissue injury following AF ablation. We demonstrate that in the acute stages post-PVAI, patients showed decreased LA wall enhancement from 24 hours to 3 months, with qualitatively distinct enhancement patterns between those two time points. We also found RF-induced scar appears to form by 3 months post-ablation with no recovery or reduction of scar after that time point. This was confirmed by similarities in LA scar percentage and consistency in size, location, and intensity of LA lesions between MRI acquired at three months post-ablation and those with later follow-up.

Acute Response

Our results indicate AF patients experience significant LA wall enhancement in the acute stages post-ablation with the majority of patients showing decreased enhancement at 3 months. Analysis of three dimensional MRI models of the LA in the acute stages post-PVAI showed distinctly unique enhancement patterns as compared with MRI scans at later time points. Acute scans showed a less intense, diffuse, and scattered enhancement pattern that partially resolved when compared with MR images at 3 months. We believe the high levels of enhancement 24 hours post-PVAI could represent

an overestimation of the necrotic scar size in the acute stages, similar to the overestimation reported with left ventricular infarct size following ischemic events.¹⁹⁻²⁴ In prior studies involving ischemic events, the authors speculate that gadolinium-enhancement of left ventricular scar decreases over time. This may occur due to involution of scar into a smaller volume, partial volume effects, and/or peri-infarct edema of the bordering scar cardiomyocytes. Furthermore, other authors have speculated that the decrease in left ventricular enhancement between 24 hours and three months could represent injured but reversible tissue in the peri-necrotic zone.²⁵ This tissue appears to heal over time and may recover myocardial function following reperfusion.²⁶

We believe the overestimation of LA enhancement in the acute stage post-PVAI could be the result of a inflammatory process induced by RF energy delivery. A transient inflammatory process causing LA edema and hemorrhage in addition to cardiomyocyte necrosis has been described in numerous animal studies involving RF catheter ablation.^{8, 10, 27} Deneke et al described an acute tissue reaction post-RFCA with distinctly different atrial tissue reactions between the first week and month post-RF ablation.²⁷ In their study, they detected zones of fresh bleeding sometimes producing confluent intramural hematoma up to 22 days after the ablation procedure, possibly due to thermal damage to smaller blood vessels with vessel wall alterations (leakage) and thrombosis. Oswald et al, also found elevated CRP levels immediately post ablation that they believed was secondary to the release of endothelial and myocardial inflammatory cytokines and increased inflammation.²⁸

The inflammatory process and increased leakage result in increased edema of the LA. A recent study by Okada et al using electron beam X-ray computed tomography (CT) demonstrated significant LA wall edema following RF ablation that self-resolved by one month following the procedure.²⁹ The non-invasive CT study has very high spatial resolution but to date can only depict the wall of the LA, and not whether or not contrast enhancement is present. Others have reported that severe LA edema

may remain even 2 months following the ablation procedure.³⁰ It has been shown that gadolinium accumulates in cardiac tissue with increased water content³¹ and enhances myocardial regions where the extracellular volume is increased, such as in conditions of inflammation, edema, and/or necrosis (9-11).³²⁻³⁴ We believe this explains the difficulty in distinguishing which processes are responsible for the MRI enhancement in the acute stages post ablation. Also, an interesting point of the Okada study was the discovery of edematous changes in the LA wall in locations remote from the PV's where RF energy was not delivered. In our study, the 24 hour MRI scans revealed hyperenhancement in locations not targeted with RF energy and remote from the pulmonary veins, including the anterior wall. The enhancement in these regions had disappeared by three months. This finding further supports the notion that inflammation could be partly responsible for the enhancement present in the 24 hour scan prior to self-resolving by three months.

An immediate post-ablation inflammatory state could also explain why some patients demonstrate early recurrences of AF in the immediate days and weeks following the procedure. Oral et al demonstrated that approximately 35% of AF patients experienced a brief episode of AF recurrence shortly after PV isolation.³⁵ They further showed that one-third of patients eventually had successful AF termination, suggesting that early recurrence was only a transient phenomenon. We speculate that although electrical isolation of the PV's is often achieved peri-procedurally, the disruption of electrical circuits could be the result of inflammation and edema and not necessarily due to cardiomyocyte necrosis. In certain patients, early recurrence of AF could possibly occur as inflammation self-resolves prior to scar formation. Continued AF recurrence following the blanking period could be the result of inadequate scar formation. Thus, whether the early AF recurrence self-resolves or continues following 3 months could be related to the location and extent of eventual LA scar formation.

Chronic Response

In our study we found that by three months post-procedure the RF-induced enhancement on MRI showed great consistency with scans acquired at 6 or 9 months. This likely represents permanent LA wall injury. In our analysis, most patients experienced only a minimal change in scar after 3 months with some patients experiencing a slight expansion of relative LA scar percentage at later follow-up. This minimal increase in scar percentage could be related to the repeatability of the approach, or secondary to volumetric changes associated with structural remodeling of the LA following restoration of sinus rhythm. The increase could also be the result of the physiologic properties of the bordering cardiomyocytes of the scar. In our study, we found that new scar detected at 6 or 9 months only existed in regions adjacent to scar seen at three months. No new scar formation occurred in regions of the LA not associated with lesions seen on MRI scans acquired at three months. The gradual expansion of LA wall scar in the chronic stage could be similar to the physiologic response reported in LV ischemic patients.³⁶⁻³⁸ Studies have shown that in patients who experienced an LV ischemic event, the cells bordering the infarct zone are significantly hypertrophied. These cells eventually outgrow the capillary network and undergo apoptosis due to inadequate oxygenation and nutrient supply.³⁶⁻³⁸ A similar pathophysiological response could explain the gradual expansion of RF-induced scar along the peri-necrotic zones following ablation of the LA.

Currently there is much debate and speculation among electrophysiologists regarding the mechanisms of AF recurrence following catheter ablation (Gerstenfeld Callans Dixit Incidence and Location of focal atrial fibrillation triggers in patients undergoing repeat pulmonary vein isolation).³⁹ One theory is that recovery of LA scar occurs allowing for resumption of electrical conduction in previously isolated PVs.³⁹⁻⁴² Our data appears to indicate that by three months post-ablation, there is no recovery or reduction in scar lesions. Indeed, there may be a small overall increase. This may signify that any recovery of electrical isolation is likely the result of inadequate scarring from the

procedure rather than resumption of electrical conduction in previously scarred atrial tissue. By understanding that any recovery of chronic lesions is minimal, this helps to focus research on elucidating the mechanisms responsible for AF recurrence following ablation. It might also be possible that individual LA substrates respond differently to RF energy than others. An increased understanding of the factors involved in RF-induced scar formation will be of immense value in determining treatment algorithms that triage AF patients to either medical or interventional therapy.

Clinical Implications

Recent advances in cardiac MRI show the potential to provide significant clinical applicability in the management and treatment of AF. The ability for practitioners to noninvasively assess PV isolation and extent of scarring using DE-MRI can potentially provide insight into the relationship between successful PV isolation and clinical outcome.

Our study shows that in the immediate stages following PVAI, the LA exhibits enhancement patterns that do not always indicate the extent and location of eventual scar formation. This may be due to transient inflammation following the procedure and during the first few months of recovery. However, comparisons of PV scar patterns at three months were very consistent to scar patterns seen at later follow up periods. This may indicate that 3 months post-PVAI is an appropriate time to acquire post-ablation DE-MRI to evaluate for pulmonary vein isolation and extent of LA wall scarring.

Cardiac MRI has the potential to help answer many of the perplexing questions regarding the basic properties of AF; including the mechanisms of AF recurrence following catheter ablation. Research is needed to correlate RF-induced scar patterns to clinical outcome as well as to determine the LA substrate properties responsible for scar formation. Increased understanding of these points may provide insight into why individual AF patients have dramatically different responses to ablation therapy.

Study Limitations

Though the trends noted are consistent among patients, the sample size for our study is small. In addition, 3D MR imaging in this study was performed on 1.5 Tesla Scanner. Significant improvements in LA wall imaging with greater spatial resolution, signal to noise ratio (SNR) and contrast to noise ratio (CNR) is expected at higher magnetic fields (3 Tesla). The difference in SNR and CNR may allow for differentiation of edema from necrotic myocardium. A second limitation regards the limited number of time points for individual patients. Yet, while the number of time points is small, there is a great degree of consistency in the results among all patients. Future work in this area should utilize a greater number of time points to explore the formation of scar in the first few months following ablation for AF.

Conclusion

RF-induced scar as measured by DE-MRI following PVAI appears to have formed by three months post-ablation. Scar patterns remain consistent in extent, location, and intensity at later follow up. At 24 hours following the procedure, DE-MRI enhancement patterns appear consistent with a transient inflammatory response that self-resolves prior to LA scar formation.

Acknowledgements

The authors gratefully acknowledge the aid of Jessiciah Windfelder in the preparation of this manuscript.

Disclosures

Doctors Edward V.R. DiBella, Eugene G. Kholmovski, and Nassir F. Marrouche are partially supported by grants from Siemens Medical Corporation and SurgiVision Corporation.

References

1. Stabile G, Bertaglia E, Senatore G, De Simone A, Zoppo F, Donnici G, Turco P, Pascotto P, Fazzari M, Vitale DF. Catheter ablation treatment in patients with drug-refractory atrial fibrillation: a prospective, multi-centre, randomized, controlled study (Catheter Ablation For The Cure Of Atrial Fibrillation Study). *Eur Heart J*. 2006;27(2):216-221.
2. Marrouche NF, Martin DO, Wazni O, Gillinov AM, Klein A, Bhargava M, Saad E, Bash D, Yamada H, Jaber W, Schweikert R, Tchou P, Abdul-Karim A, Saliba W, Natale A. Phased-array intracardiac echocardiography monitoring during pulmonary vein isolation in patients with atrial fibrillation: impact on outcome and complications. *Circulation*. 2003;107(21):2710-2716.
3. Marrouche NF, Dresing T, Cole C, Bash D, Saad E, Balaban K, Pavia SV, Schweikert R, Saliba W, Abdul-Karim A, Pisano E, Fanelli R, Tchou P, Natale A. Circular mapping and ablation of the pulmonary vein for treatment of atrial fibrillation: impact of different catheter technologies. *Journal of the American College of Cardiology*. 2002;40(3):464-474.
4. Verma A, Marrouche NF, Natale A. Pulmonary vein antrum isolation: intracardiac echocardiography-guided technique. *Journal of cardiovascular electrophysiology*. 2004;15(11):1335-1340.
5. Haissaguerre M, Jais P, Shah DC, Takahashi A, Hocini M, Quiniou G, Garrigue S, Le Mouroux A, Le Metayer P, Clementy J. Spontaneous initiation of atrial fibrillation by ectopic beats originating in the pulmonary veins. *The New England journal of medicine*. 1998;339(10):659-666.
6. Pappone C, Rosanio S, Oreto G, Tocchi M, Gugliotta F, Vicedomini G, Salvati A, Dicandia C, Mazzone P, Santinelli V, Gulletta S, Chierchia S. Circumferential radiofrequency ablation of pulmonary vein ostia: A new anatomic approach for curing atrial fibrillation. *Circulation*. 2000;102(21):2619-2628.
7. Jais P, Weerasooriya R, Shah DC, Hocini M, Macle L, Choi KJ, Scavee C, Haissaguerre M, Clementy J. Ablation therapy for atrial fibrillation (AF): past, present and future. *Cardiovasc Res*. 2002;54(2):337-346.
8. Dickfeld T, Kato R, Zviman M, Lai S, Meininger G, Lardo AC, Roguin A, Blumke D, Berger R, Calkins H, Halperin H. Characterization of radiofrequency ablation lesions with gadolinium-enhanced cardiovascular magnetic resonance imaging. *Journal of the American College of Cardiology*. 2006;47(2):370-378.
9. Deneke T, Khargi K, Lemke B, Lawo T, Lindstaedt M, Germing A, Brodherr T, Bosche L, Mugge A, Laczkovics A, Grewe PH, Fritz M. Intra-operative cooled-tip radiofrequency linear atrial ablation to treat permanent atrial fibrillation. *Eur Heart J*. 2007;28(23):2909-2914.
10. Aupperle H, Doll N, Walther T, Ullmann C, Schoon HA, Wilhelm Mohr F. Histological findings induced by different energy sources in experimental atrial ablation in sheep. *Interact Cardiovasc Thorac Surg*. 2005;4(5):450-455.
11. Huang SK, Bharati S, Graham AR, Lev M, Marcus FI, Odell RC. Closed chest catheter desiccation of the atrioventricular junction using radiofrequency energy--a new method of catheter ablation. *Journal of the American College of Cardiology*. 1987;9(2):349-358.
12. Santiago T, Melo JQ, Gouveia RH, Martins AP. Intra-atrial temperatures in radiofrequency endocardial ablation: histologic evaluation of lesions. *The Annals of thoracic surgery*. 2003;75(5):1495-1501.
13. Peters DC, Wylie JV, Hauser TH, Kissinger KV, Botnar RM, Essebag V, Josephson ME, Manning WJ. Detection of pulmonary vein and left atrial scar after catheter ablation with three-

dimensional navigator-gated delayed enhancement MR imaging: initial experience. *Radiology*. 2007;243(3):690-695.

14. MCGann CJ, Kholmovski EG, Oakes RS, Blauer JJE, Daccarett M, Segerson NM, Airey KJ, Akoum N, Fish EN, Badger TJ, Di Bella EVR, Parker D, MacLeod RS, Marrouche NF. New magnetic resonance imaging based method to define the extent of left atrial wall injury after the ablation of atrial fibrillation. *JACC*. 2008;[In Press].
15. McGann C, Kholmovski EG, Oakes RS, Di Bella EVR, MacLeod RS, Fish E, Daccarett M, Segerson NM, Marrouche NF. Magnetic Resonance Imaging Detects Chronic Left Atrial Wall Injury Post Ablation of Atrial Fibrillation. Paper presented at: Scientific Sessions - AHA 2007, 2007; Orlando, Florida.
16. Ouyang F, Antz M, Ernst S, Hachiya H, Mavrakis H, Deger FT, Schaumann A, Chun J, Falk P, Hennig D, Liu X, Bansch D, Kuck KH. Recovered pulmonary vein conduction as a dominant factor for recurrent atrial tachyarrhythmias after complete circular isolation of the pulmonary veins: lessons from double Lasso technique. *Circulation*. 2005;111(2):127-135.
17. Ouyang F, Ernst S, Chun J, Bansch D, Li Y, Schaumann A, Mavrakis H, Liu X, Deger FT, Schmidt B, Xue Y, Cao J, Hennig D, Huang H, Kuck KH, Antz M. Electrophysiological findings during ablation of persistent atrial fibrillation with electroanatomic mapping and double Lasso catheter technique. *Circulation*. 2005;112(20):3038-3048.
18. Kanj MH, Wazni O, Fahmy T, Thal S, Patel D, Elay C, Di Biase L, Arruda M, Saliba W, Schweikert RA, Cummings JE, Burkhardt JD, Martin DO, Pelargonio G, Dello Russo A, Casella M, Santarelli P, Potenza D, Fanelli R, Massaro R, Forleo G, Natale A. Pulmonary vein antral isolation using an open irrigation ablation catheter for the treatment of atrial fibrillation: a randomized pilot study. *Journal of the American College of Cardiology*. 2007;49(15):1634-1641.
19. Saeed M, Wendland MF, Masui T, Higgins CB. Reperfused myocardial infarctions on T1- and susceptibility-enhanced MRI: evidence for loss of compartmentalization of contrast media. *Magn Reson Med*. 1994;31(1):31-39.
20. Saeed M, Lund G, Wendland MF, Bremerich J, Weinmann H, Higgins CB. Magnetic resonance characterization of the peri-infarction zone of reperfused myocardial infarction with necrosis-specific and extracellular nonspecific contrast media. *Circulation*. 2001;103(6):871-876.
21. Judd RM, Lugo-Olivieri CH, Arai M, Kondo T, Croisille P, Lima JA, Mohan V, Becker LC, Zerhouni EA. Physiological basis of myocardial contrast enhancement in fast magnetic resonance images of 2-day-old reperfused canine infarcts. *Circulation*. 1995;92(7):1902-1910.
22. Schaefer S, Malloy CR, Katz J, Parkey RW, Buja LM, Willerson JT, Peshock RM. Gadolinium-DTPA-enhanced nuclear magnetic resonance imaging of reperfused myocardium: identification of the myocardial bed at risk. *Journal of the American College of Cardiology*. 1988;12(4):1064-1072.
23. Saeed M, Bremerich J, Wendland MF, Wytenbach R, Weinmann HJ, Higgins CB. Reperfused myocardial infarction as seen with use of necrosis-specific versus standard extracellular MR contrast media in rats. *Radiology*. 1999;213(1):247-257.
24. Rochitte CE, Lima JA, Bluemke DA, Reeder SB, McVeigh ER, Furuta T, Becker LC, Melin JA. Magnitude and time course of microvascular obstruction and tissue injury after acute myocardial infarction. *Circulation*. 1998;98(10):1006-1014.
25. Kim RJ, Fieno DS, Parrish TB, Harris K, Chen EL, Simonetti O, Bundy J, Finn JP, Klocke FJ, Judd RM. Relationship of MRI delayed contrast enhancement to irreversible injury, infarct age, and contractile function. *Circulation*. 1999;100(19):1992-2002.

26. Rogers WJ, Jr., Kramer CM, Geskin G, Hu YL, Theobald TM, Vido DA, Petruolo S, Reichek N. Early contrast-enhanced MRI predicts late functional recovery after reperfused myocardial infarction. *Circulation*. 1999;99(6):744-750.
27. Deneke T, Khargi K, Muller KM, Lemke B, Mugge A, Laczkovics A, Becker AE, Grewe PH. Histopathology of intraoperatively induced linear radiofrequency ablation lesions in patients with chronic atrial fibrillation. *Eur Heart J*. 2005;26(17):1797-1803.
28. Oswald H, Gardiwal A, Lissel C, Yu H, Klein G. Difference in humoral biomarkers for myocardial injury and inflammation in radiofrequency ablation versus cryoablation. *Pacing Clin Electrophysiol*. 2007;30(7):885-890.
29. Okada T, Yamada T, Murakami Y, Yoshida N, Ninomiya Y, Shimizu T, Toyama J, Yoshida Y, Ito T, Tsuboi N, Kondo T, Inden Y, Hirai M, Murohara T. Prevalence and severity of left atrial edema detected by electron beam tomography early after pulmonary vein ablation. *Journal of the American College of Cardiology*. 2007;49(13):1436-1442.
30. Steel KE, Roman-Gonzalez J, O'Bryan CL. Images in cardiovascular medicine. Severe left atrial edema and heart failure after atrial fibrillation ablation. *Circulation*. 2006;113(12):e659.
31. Adzhamli IK, Jolesz FA, Bleier AR, Mulkern RV, Sandor T. The effect of gadolinium DTPA on tissue water compartments in slow- and fast-twitch rabbit muscles. *Magn Reson Med*. 1989;11(2):172-181.
32. Bogaert J, Taylor AM, Van Kerckhove F, Dymarkowski S. Use of inversion recovery contrast-enhanced MRI for cardiac imaging: spectrum of applications. *AJR Am J Roentgenol*. 2004;182(3):609-615.
33. Aso H, Takeda K, Ito T, Shiraishi T, Matsumura K, Nakagawa T. Assessment of myocardial fibrosis in cardiomyopathic hamsters with gadolinium-DTPA enhanced magnetic resonance imaging. *Invest Radiol*. 1998;33(1):22-32.
34. Friedrich MG, Strohm O, Schulz-Menger J, Marciniak H, Luft FC, Dietz R. Contrast media-enhanced magnetic resonance imaging visualizes myocardial changes in the course of viral myocarditis. *Circulation*. 1998;97(18):1802-1809.
35. Oral H, Knight BP, Ozaydin M, Tada H, Chugh A, Hassan S, Scharf C, Lai SW, Greenstein R, Pelosi F, Jr., Strickberger SA, Morady F. Clinical significance of early recurrences of atrial fibrillation after pulmonary vein isolation. *Journal of the American College of Cardiology*. 2002;40(1):100-104.
36. Gu X, Cheng L, Chueng WL, Yao X, Liu H, Qi G, Li M. Neovascularization of ischemic myocardium by newly isolated tannins prevents cardiomyocyte apoptosis and improves cardiac function. *Mol Med*. 2006;12(11-12):275-283.
37. Kocher AA, Schuster MD, Szabolcs MJ, Takuma S, Burkhoff D, Wang J, Homma S, Edwards NM, Itescu S. Neovascularization of ischemic myocardium by human bone-marrow-derived angioblasts prevents cardiomyocyte apoptosis, reduces remodeling and improves cardiac function. *Nat Med*. 2001;7(4):430-436.
38. Cheng W, Kajstura J, Nitahara JA, Li B, Reiss K, Liu Y, Clark WA, Krajewski S, Reed JC, Olivetti G, Anversa P. Programmed myocyte cell death affects the viable myocardium after infarction in rats. *Exp Cell Res*. 1996;226(2):316-327.
39. Gerstenfeld EP, Callans DJ, Dixit S, Zado E, Marchlinski FE. Incidence and location of focal atrial fibrillation triggers in patients undergoing repeat pulmonary vein isolation: implications for ablation strategies. *Journal of cardiovascular electrophysiology*. 2003;14(7):685-690.
40. Katritsis DG, Ellenbogen KA, Panagiotakos DB, Giazitzoglou E, Karabinos I, Papadopoulos A, Zambartas C, Anagnostopoulos CE. Ablation of superior pulmonary veins compared to

ablation of all four pulmonary veins. *Journal of cardiovascular electrophysiology*. 2004;15(6):641-645.

41. Cappato R, Negroni S, Pecora D, Bentivegna S, Lupo PP, Carolei A, Esposito C, Furlanello F, De Ambroggi L. Prospective assessment of late conduction recurrence across radiofrequency lesions producing electrical disconnection at the pulmonary vein ostium in patients with atrial fibrillation. *Circulation*. 2003;108(13):1599-1604.
42. Nanthakumar K, Plumb VJ, Epstein AE, Veenhuyzen GD, Link D, Kay GN. Resumption of electrical conduction in previously isolated pulmonary veins: rationale for a different strategy? *Circulation*. 2004;109(10):1226-1229.

Figures and Tables

Figure Legends

Figure 1. Three dimensional delayed enhancement MRI analysis of scar patterns in a single patient at 24 hours and 3 months post pulmonary vein antrum isolation. Twenty-four hour MRI shows diffuse enhancement patterns with a substantial reduction in the detected scar between the left lateral and posterior wall at the 3 month scan. At 3 months, LA scar patterns appear to be in well-demarcated scar borders along the posterior wall and around the PV antrum. Comparison of 3D images between these two time points demonstrate scar changes.

Figure 2. Shows MRI scans acquired at 3 months (top) and 6 months (bottom) in a single patient. There are consistent scar patterns and intensity in the two dimensional MRI slices (left) at both time points. Three dimensional reconstructions in three separate views (posterior, left lateral and right lateral) show RF induced scarring that is consistent between the three month scan and the six month scan.

Figure 3. Change in scar in patients from 24 hours to 3 months (Group 1) and from 3 months to latest follow-up at 6 or 9 months (Group 2). An overall reduction is seen in patients from 24 hours to three months, while a small increase is seen in patients from 3 months to the time of latest follow-up. The between the two groups difference was statistically significant ($p = 0.048$, Wilcoxon Ranked Sums Test).

Figure 4. Qualitative comparison of LA posterior wall scar patterns between 24 hours and 3 months (Patient 1) and 3 months and 6 months (Patient 2). In patient 1, the 24 hour scar patterns appear diffuse and distinct from those seen at 3 months. Further, there is a considerable reduction in scar (which is notable in the lower right posterior wall). In Patient 2, scar patterns are consistent in size and location between 3 and 6 months, showing little apparent change or recovery. The graph at right illustrates the statistical significance ($p < 0.001$, Wilcoxon Ranked Sums test) of similar LA scar patterns in the acute versus chronic stages following pulmonary vein antrum isolation. The qualitative relationship between scar at chronic time points is much greater than that seen during acute time points.

Figure 5. Relationship between detected scar formations at 24 hours and 3 months (left) or 3 months and later follow-up (6 or 9 months; right). No correlation is seen between the extent of detected injury at 24 hours and 3 months, while a strong correlation is seen between detected injury at 3 months and later follow-up.

Tables

Table 1. Patient Demographics

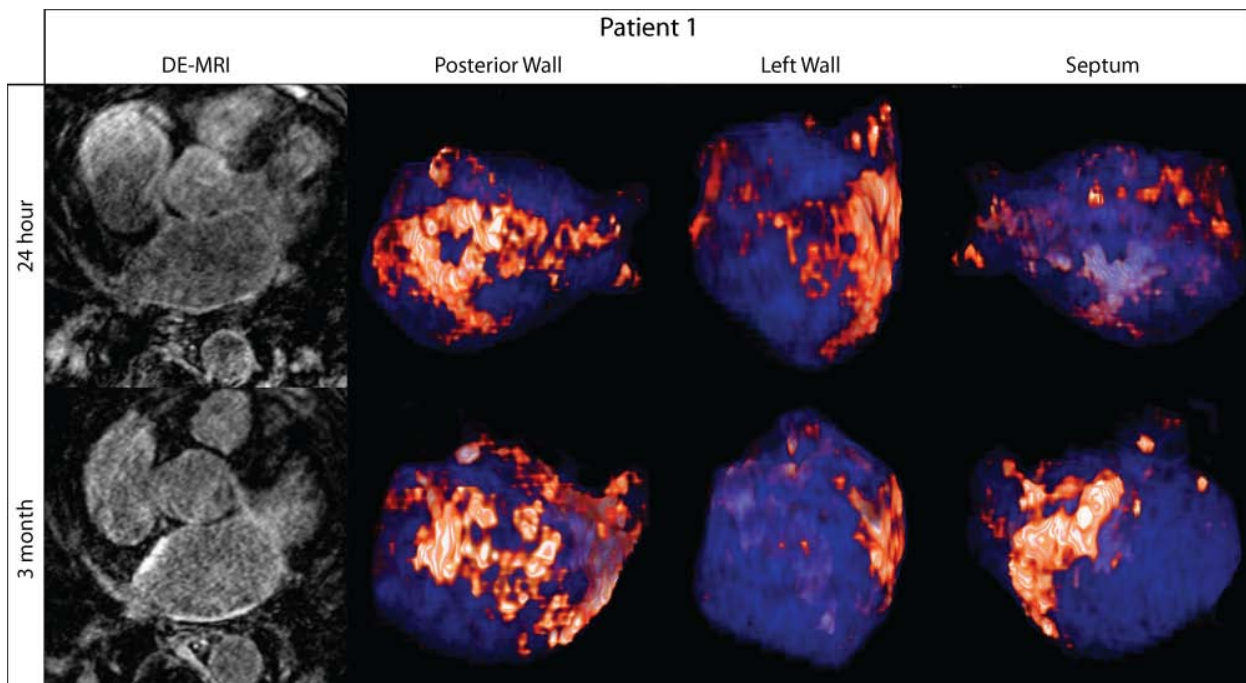
	Overall (n = 25) *	Group 1 (n = 10)	Group 2 (n = 16)	P-Value †
Age (Years)				
Type of Atrial Fibrillation				
Paroxysmal	16 (61.5%)	5 (50.0%)	12 (75.0%)	0.32
Persistent	8 (30.8%)	5 (50.0%)	3 (18.8%)	
Longstanding Persistent	1 (3.8%)	-	1 (6.3%)	
Gender				
Female	12 (48%)	7 (70%)	5 (31.3%)	0.025
Male	13 (52%)	3 (30%)	11 (68.6%)	
Hypertension	10 (38.5%)	5 (50%)	6 (37.5%)	0.412
Diabetes	3 (11.5%)	1 (10%)	2 (12.5%)	0.677
Coronary Artery Disease	-	-	-	-
History of Smoking	6 (23.1%)	3 (30%)	3 (18.8%)	0.420
Valve Surgery	1 (3.8%)	-	1 (6.3%)	0.615
Myocardial Infarct	-	-	-	-
Congestive Heart Failure	1 (3.8%)	-	1 (6.3%)	0.640

* One patient received scans at 24 hours, 3 months and 6 months post ablation. As a result, the patient data has been included in both Group 1 and Group 2.

† Fischer Exact Test between Group 1 and Group 2. Comparison included 26 cases.

Figures

Figure 1. Three dimensional delayed enhancement MRI analysis of scar patterns in a single patient at 24 hours and 3 months post pulmonary vein antrum isolation. Twenty-four hour MRI shows diffuse enhancement patterns with a substantial reduction in the detected scar between the left lateral and posterior wall at the 3 month scan. At 3 months, LA scar patterns appear to be in well-demarcated scar borders along the posterior wall and around the PV antrum. Comparison of 3D images between these two time points demonstrate scar changes.



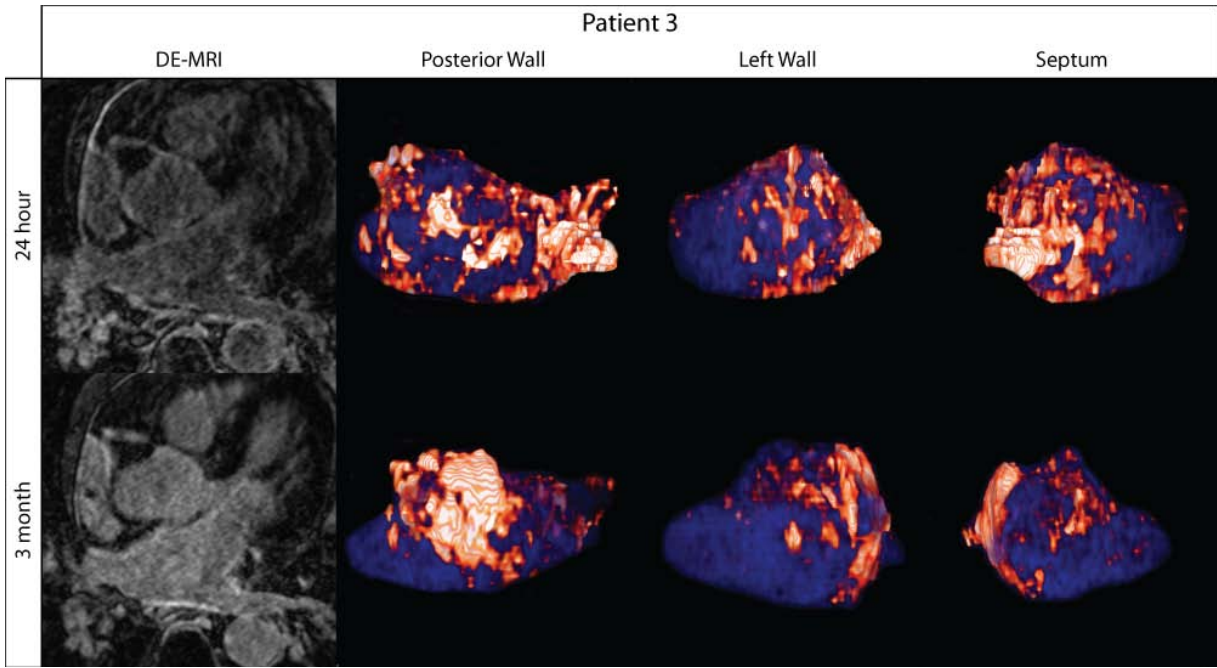
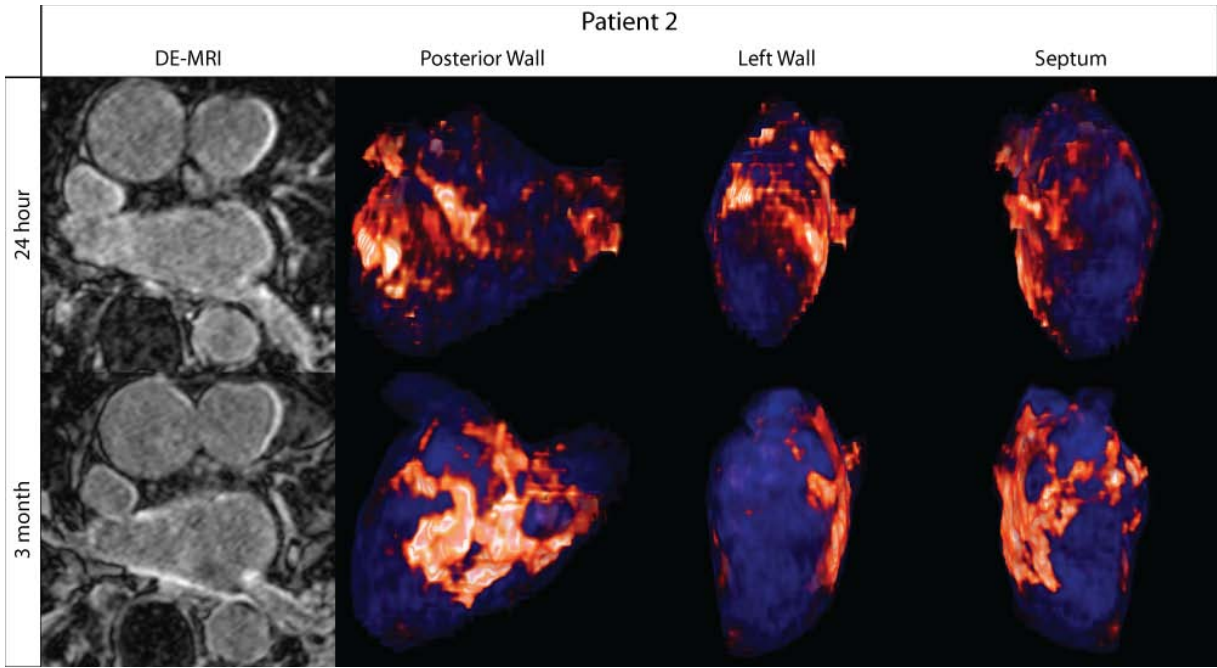
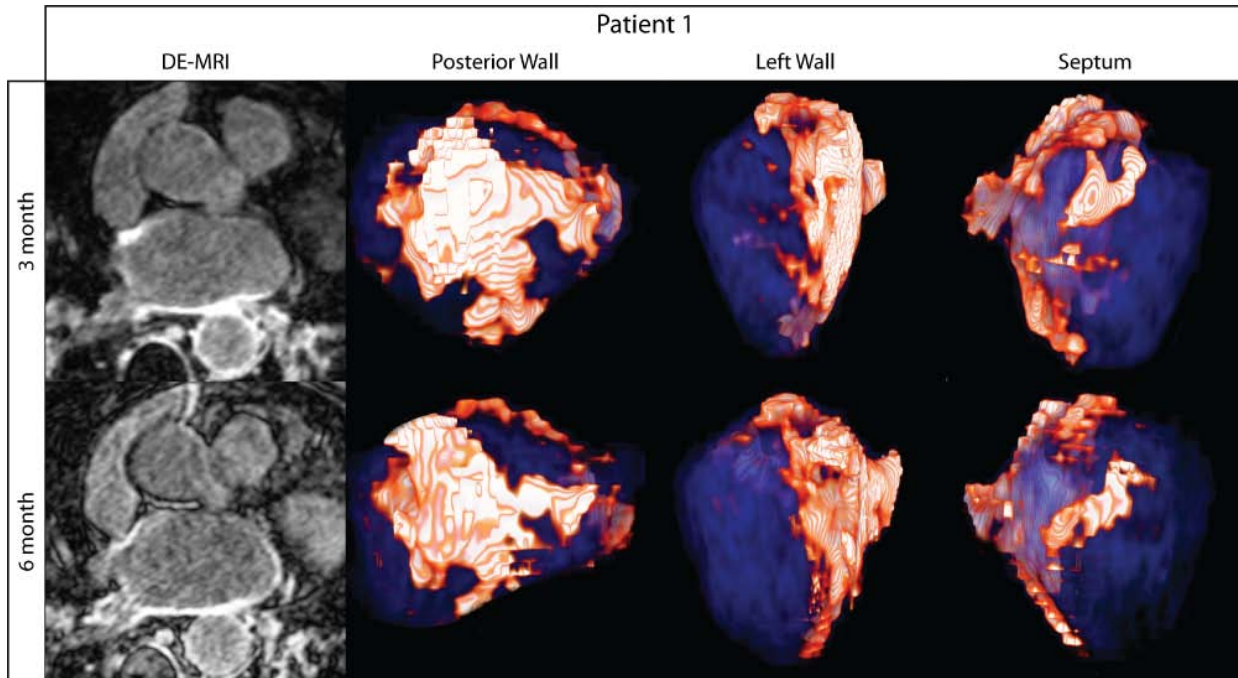


Figure 2. Shows MRI scans acquired at 3 months (top) and 6 months (bottom) in a single patient. There are consistent scar patterns and intensity in the two dimensional MRI slices (left) at both time points. Three dimensional reconstructions in three separate views (posterior, left lateral and right lateral) show RF induced scarring that is consistent between the three month scan and the six month scan.



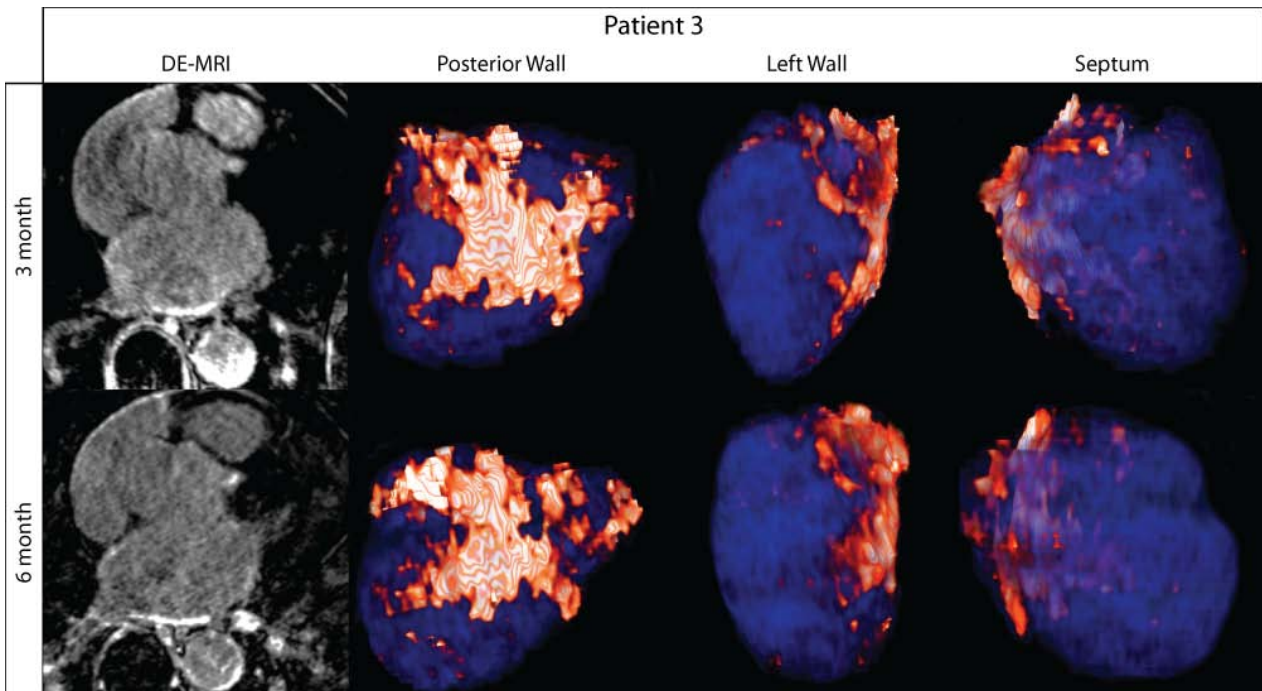
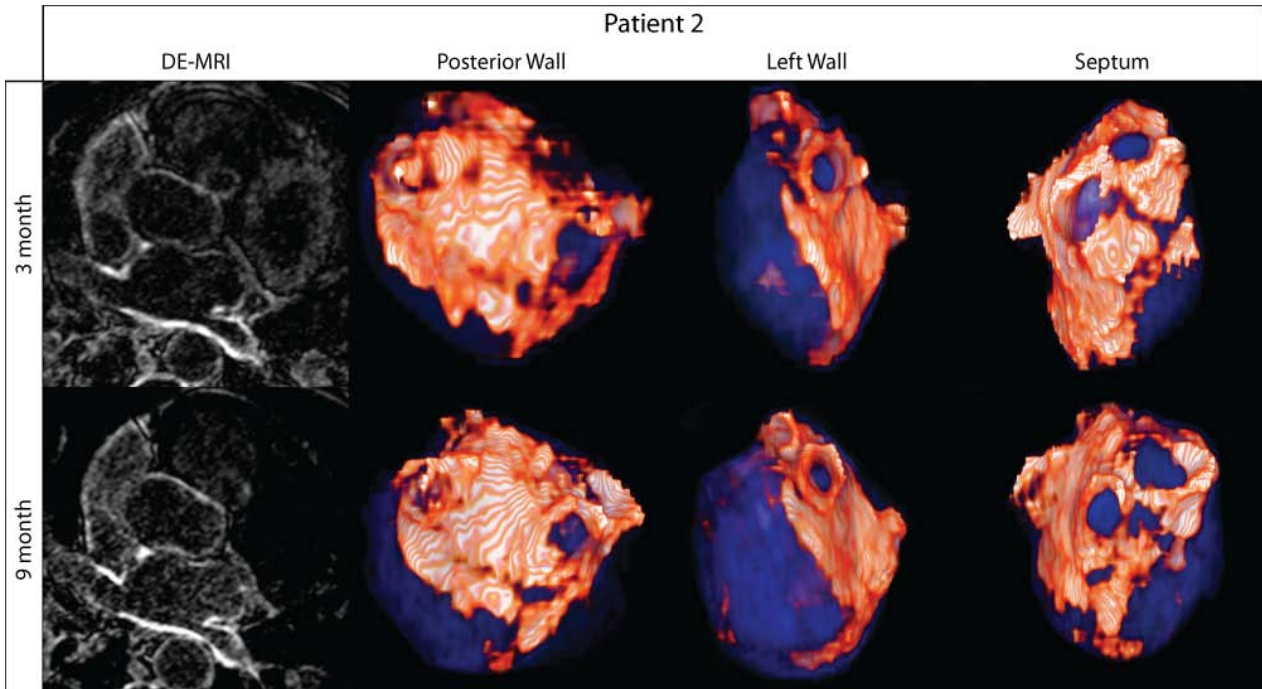


Figure 3. Change in scar in patients from 24 hours to 3 months (Group 1) and from 3 months to latest follow-up at 6 or 9 months (Group 2). An overall reduction is seen in patients from 24 hours to three months, while a small increase is seen in patients from 3 months to the time of latest follow-up. The between the two groups difference was statistically significant ($p = 0.048$, Wilcoxon Ranked Sums Test).

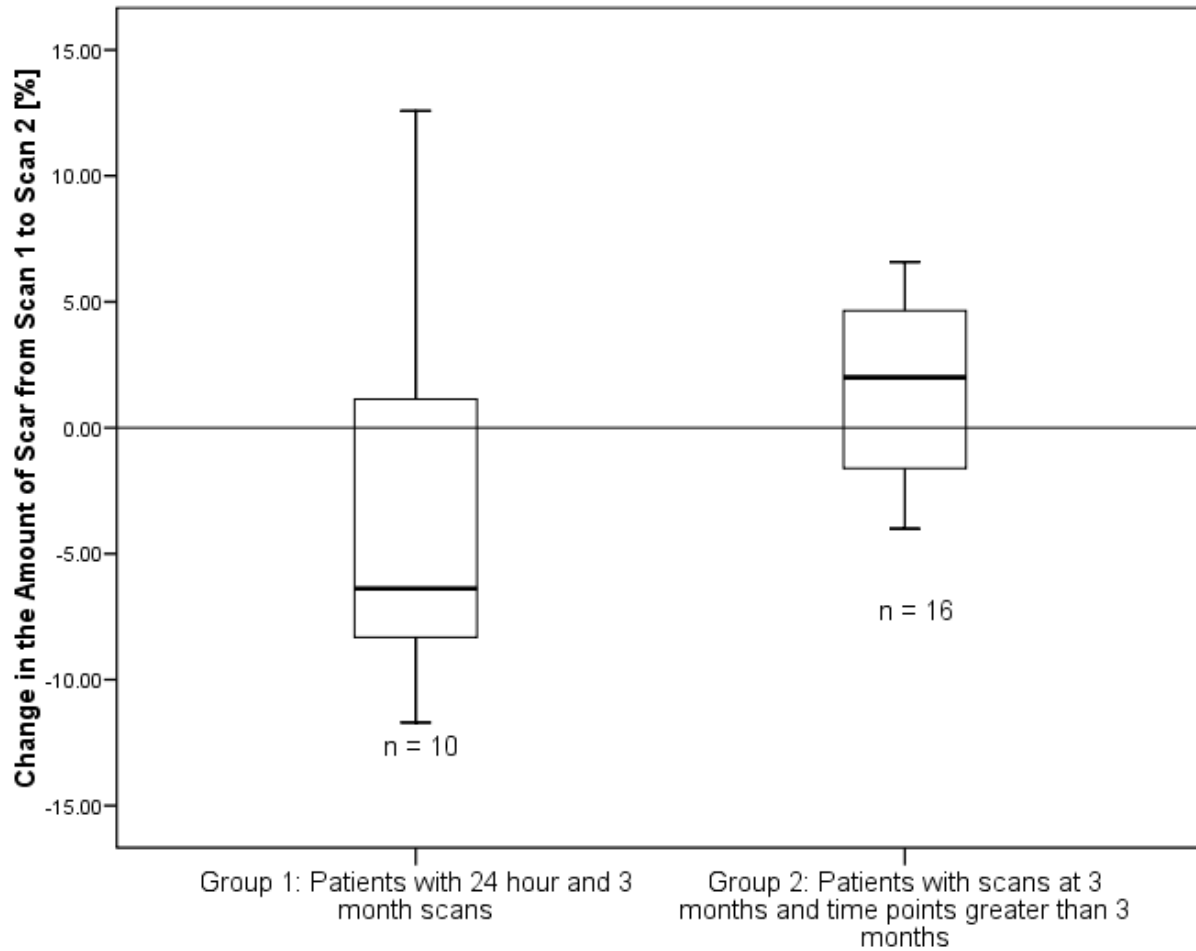


Figure 4. Qualitative comparison of LA posterior wall scar patterns between 24 hours and 3 months (Patient 1) and 3 months and 6 months (Patient 2). In patient 1, the 24 hour scar patterns appear diffuse and distinct from those seen at 3 months. Further, there is a considerable reduction in scar (which is notable in the lower right posterior wall). In Patient 2, scar patterns are consistent in size and location between 3 and 6 months, showing little apparent change or recovery. The graph at right illustrates the statistical significance ($p < 0.001$, Wilcoxon Ranked Sums test) of similar LA scar patterns in the acute versus chronic stages following pulmonary vein antrum isolation. The qualitative relationship between scar at chronic time points is much greater than that seen during acute time points.

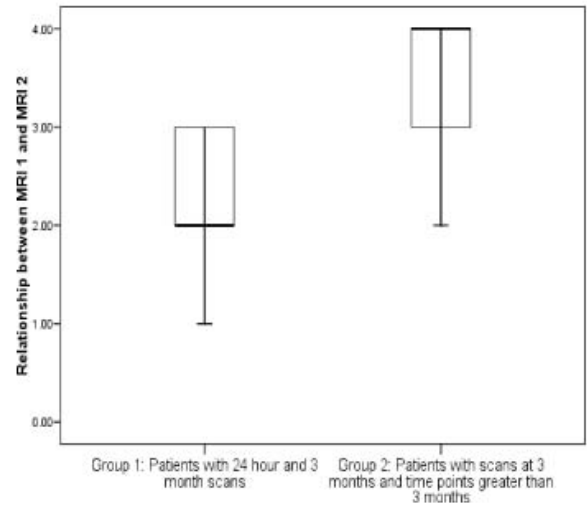
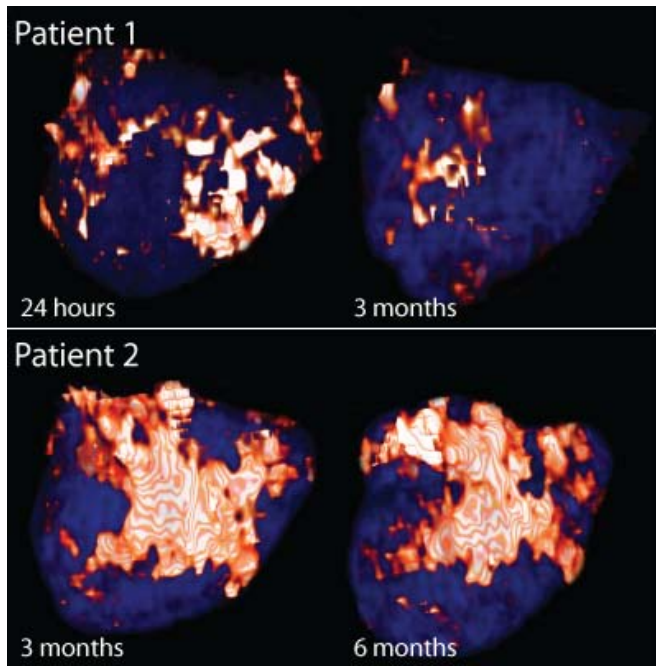
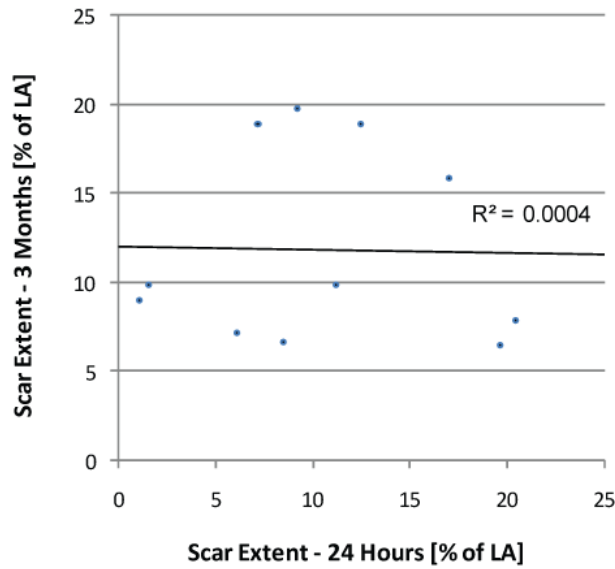


Figure 5. Relationship between detected scar formations at 24 hours and 3 months (left) or 3 months and later follow-up (6 or 9 months; right). No correlation is seen between the extent of detected injury at 24 hours and 3 months, while a strong correlation is seen between detected injury at 3 months and later follow-up.

Scar Extent at 24 Hours and 3 Months



Scar Extent at 3 Months and 6 or 9 Months

